Wideband Dual-Polarized 1-Bit Unit-cell Design for mmWave Reconfigurable Intelligent Surface

Gabriel G. Machado*†, M. Ali Babar Abbasi†, Adrian McKernan†, Chao Gu†, Dmitry Zelenchuk†
*School of Engineering, Ulster University, Belfast, UK, g.machado@ulster.ac.uk
†Centre for Wireless Innovation, Queen's University Belfast, Belfast, UK, d.zelenchuk@qub.ac.uk

***Abstract*—This study presents a novel reflective unit-cell with wideband characteristics at millimeter-wave (mmWave) bands for application in Reconfigurable Intelligent Surfaces (RIS). The proposed unit-cell design demonstrates through full-wave simulations a superior bandwidth performance over the 26.50–29.45 GHz, targeting the n257 band of mmWave 5G. The design was created for dual-polarization operation, each controlled by a p-i-n diode to realise a 1-bit RIS. The design achieves impressive performance, maintaining a phase difference error within ±20 degrees across most of the 3 GHz bandwidth while reflecting over 80% of the energy. The increased reflectivity minimizes losses, while precise phase control improves beam pointing accuracy, crucial in low-complexity 1-bit systems. Numerical simulations also indicate that this unit-cell performs effectively in a 6-layer PCB stack-up. A comparison with state-of-the-art unit-cells for RIS design is also presented, demonstrating the advantages of the proposed design in terms of bandwidth, dual-polarization operation, and phase accuracy.**

***Index Terms*—antennas, mmWave, RIS, unit-cell, reconfigurable**

I. Introduction

In recent years, Reconfigurable Intelligent Surfaces (RIS) have emerged as the technology with the potential to revolutionize wireless communication systems. RIS can intelligently control and manipulate radio waves to redirect the energy from a base-station (BS) to a user equipment (UE) not in its line of sight (LoS), as illustrated in Fig. 1. By strategically adjusting the phase and amplitude of reflected signals, RIS-aided channels offer unique capabilities for enhancing the performance of wireless networks, including improved signal coverage, higher data rates, and energy efficient gains [1]–[3]. This technology has found a potential application in the millimeter-wave domain, which suffers the most from high free-space path loss (FSPL) and poor link connection when obstacles block LoS compared to any other existing commercial wireless technology [4], [5].

A RIS is a reconfigurable metasurface, employing meta-atoms loaded with varactors or p-i-n diodes [6], [7] to form a unit-cell. The unit-cell's design parameters, such as shape, dimensions and thickness, determine the RIS's overall performance, including its operational bandwidth, phase range, and polarization versatility. Therefore, the development of efficient and wideband unit-cells plays a crucial role on its practical use, keeping in mind that 5G mmWave band allocations are region-specific in global context [8].

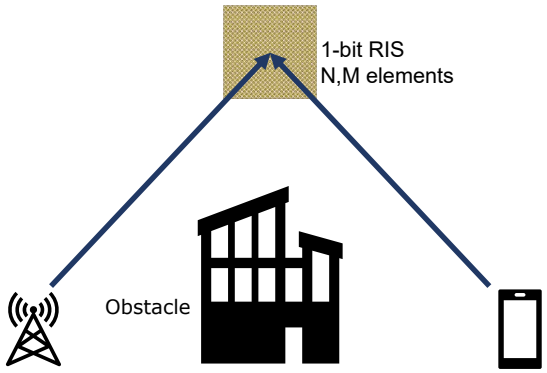

Fig. 1. Illustration of a scenario where a RIS can provide a link between the BS and UE where blind-spots occur due to the presence of obstacles.

RIS for mmWave applications, however, are challenging devices to realize due to the complexity of the design, including dimensions, bias network, and control architecture, usually achieved by shift registers and/or field programmable gate arrays (FPGAs). In [9], a group from Samsung developed a 1-bit 29 GHz dual polarized RIS with a wide angle of incidence insensitivity, but with a narrow bandwidth within the n257 band. In [10] the authors developed a 2-bit 29 GHz RIS and proposed an improved path-loss model for RIS-aided mmWave channels. Although their surface presented a bandwidth limitation, similar to [9], and single polarization, a 2-bit RIS has an improved quantization error when compared to the single-bit counterpart. A well-regarded work in mmWave RIS [11], demonstrated a 1-bit RIS with a working frequency centred at 27.5 GHz, attempting to cover the n257 band, however, improvements can still be made regarding loss and bandwidth of the unit-cell. Moreover, in [12], where a 26.25 GHz 2-bit RIS is presented, the phase-shift bandwidth is also limited.

Contribution – This paper presents the design and numerical analysis of a novel wideband 1-bit unit-cell tailored for mmWave RIS applications controlled by a p-i-n diode. The proposed unit-cell works within the $26.5 - 29$ GHz band with an error of up to $\pm 10°$, around the required $180°$ phase shift for 1-bit RIS operation, and below $20°$ between $29.00 - 29.45$ GHz. Notably, different from previous works, this unit-cell is capable of covering the entire n257 band whilst maintaining dual-polarization operation, with a low loss on both states of operation of the p-i-n diode.

II. Unit-cell design

The unit-cell is patterned on a 1.52 mm thick Rogers 4003C substrate ($\epsilon_r = 3.4$ and $\tan\delta = 0.0027$) coated with 35 μm copper clad. Both vertical and horizontal unit-cells are controlled by a MADP-000907-14020P p-i-n diode. For maximum simulation accuracy, the LRC characteristics of the p-i-n diode were measured in Queen's University Belfast facilities by using a microstrip line and fitting the curves to Keysight Pathwave Advances Design Software (ADS). The fitted parameters, which showed a good agreement with what is presented in the literature for this frequency range [9], and equivalent circuit forward and reverse bias configuration are shown in Fig. 2. Moreover, for both biasing purposes and bandwidth enhancement, each unit-cell has two L0201R82AHSTR\500 RF chokes with a self-resonance at 28 GHz. At this frequency, the RF choke behaves as a parallel LRC tank with values $L_{ind} = 820$ pH, $R_{ind} = 4050\ \Omega$ and $C_{ind} = 13.12$ fF, respectively.

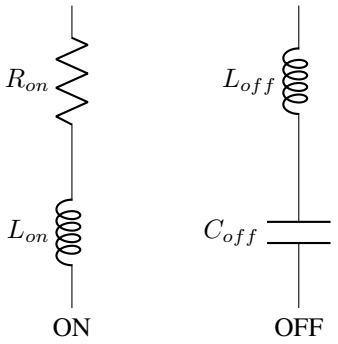

Fig. 2. MADP-000907-14020P equivalent circuit and LRC values for the forward and reverse bias configurations on the left and right, respectively.

The unit-cells are depicted in Fig. 3 along with their dimensions. The blue components in the centre of each cell represent the p-i-n diodes, whereas those following the circumference are the RF inductors. The landing pads were designed to accommodate the 0201 components as per the instructions on their datasheet.

Two 'T' shaped monopoles in Fig. 3 construct a dipole, and these dipoles are active elements depending on the orientation of the electric field. These are biased by the auxiliary elements which are isolated by the RF chokes.

Two major concerns when designing an RIS are to obtain a good reflection coefficient whilst keeping the phase difference between states as close to the requirements for a particular quantization as possible. In our case, a 1-bit RIS requires a phase difference of 180° between forward and reverse bias states. Maintaining this reduces the inevitable quantization error, which is already relevant for 1-bit architectures.

Therefore, the unit-cell was optimized by carefully selecting substrate thickness, dimension of the elements and placement of the vias, discussed in the next session of this paper.

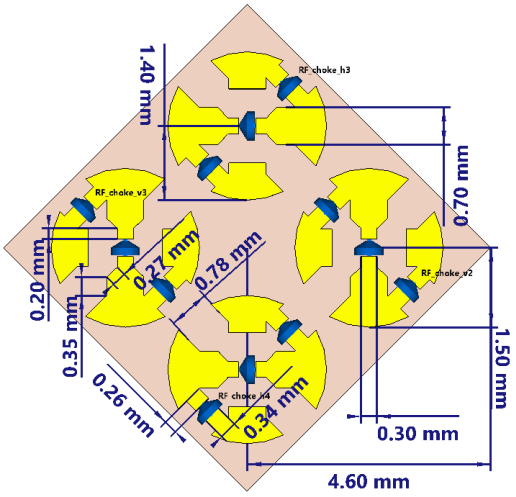

Fig. 3. Proposed unit-cell design and dimensions.

III. Numerical Analysis

The unit-cell was designed in CST Microwave Studio 2023, where unit-cell boundary condition was chosen to obtain an infinite periodic surface. A Floquet port was used to excite the unit-cell, and the reference plane was moved to the surface of the copper elements to obtain the accurate phase shift on the top of the unit-cell. The practical scenario of this unit-cell is considered right at this design stage. The planned angle of incidence at the RIS is 30° and therefore the unit-cell was optimized to obtain its best performance at this angle. The results for the magnitude of the reflection coefficient for both polarizations are shown in Fig. 4.

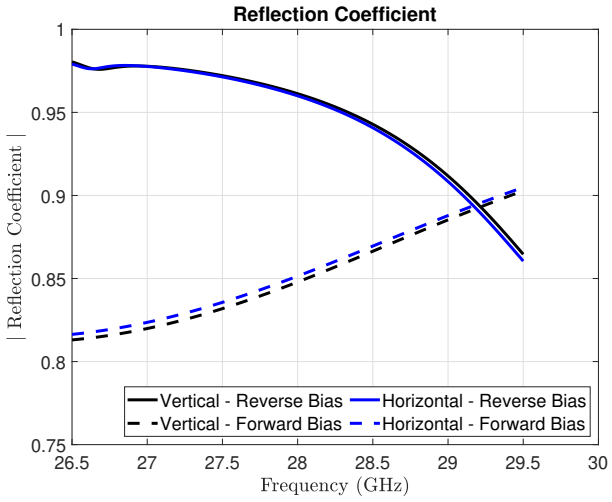

Fig. 4. Simulated magnitude of the reflection coefficient for vertical and horizontal polarizations.

We observe that in the reverse bias state, the unit-cell reflects over 90% (≥ -0.91 dB) of the impinged signal almost in its entire band of operation. Due to the resistance present in its forward bias configuration, previously shown in Fig. 2, the reflection is reduced, but it is maintained over

80% (≥ -1.8 dB). Equally important to the performance of a mmWave RIS, the phase difference between forward and reverse bias states is depicted in Fig. 5 for 30° incidence.

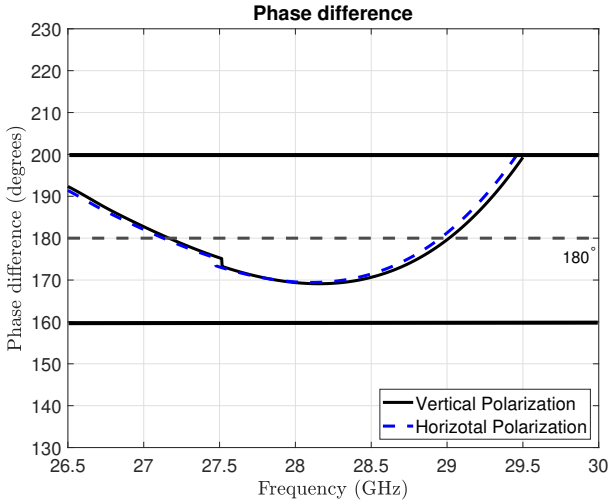

Fig. 5. Simulated phase difference between forward and reverse bias states.

The numerical results show an excellent performance achieved by the unit-cell, where less than $\pm 10°$ difference is observed between $26.5 - 29$ GHz, increasing to $< 20°$ at 29.5 GHz. This helps to mitigate part of the quantization error for 1-bit arrays [13], by means of beam pointing accuracy.

The bandwidth is achieved not only by the RF substrate thickness and tweaking the dimensions of the unit-cell, but also due to the influence of the inductors and careful placement of the vias. Fig. 6 shows the current distribution for vertically and horizontally polarized waves for both forward and reverse polarizations. The computed results show that, at its active polarization, the vias responsible for the biasing of the p-i-n diodes have a small current distributed alongside their structures. This is achieved by iterative simulations to find the location on the biasing patches where the potential difference between the element and the biasing ground was minimal.

Moreover, after locating the ideal location, we observed in our computations that the frequency response of the unit-cell is virtually unchanged when the PCB stack-up is changed. As a consequence, the simulations could be significantly simplified for its optimization stage. This is demonstrated in the results shown in Fig. 7, which demonstrates the unit-cell operating at 30° incidence for 2, and 6 layers (planned for our full RIS design) PCB stack-up. The stack-up consists of one 1.52 mm RO4003C core, 95 μm S1000-2MB prepreg ($\epsilon_r = 4.6$, $\tan\delta = 0.018$), and 1.5 mm FR-4 core ($\epsilon_r = 4.5$, $\tan\delta = 0.02$) to obtain a symmetric design and reduce bow and twist when the RIS is manufactured.

The results show small differences between PCB stack-ups, but the overall behavior and performance of the unit-cell are maintained, showing the robustness of the design.

Finally, Table I compares our work with the previously mentioned state-of-the-art. It highlights the bandwidth and loss ($\min(\Gamma)$) advantages presented by this unit-cell design, and its potential for RIS development. In [9], the authors did not define a bandwidth, and therefore we used the same error of $\pm 20°$ as it was the benchmark for our work. Moreover, for the works in [10], [12], where a 2-bit unit cell design is present, the phase error is not determined by the authors for

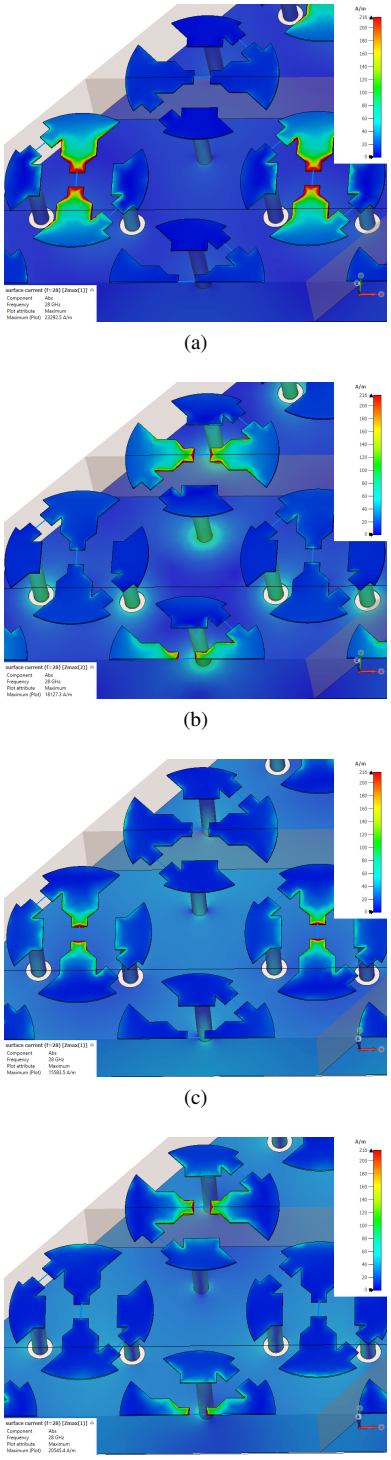

(a) (b) (c) (d)

Fig. 6. (Surface current distribution for reverse bias state (a) vertical polarization, (b) horizontal polarization, and forward bias (c) vertical polarization, (d) horizontal polarization.

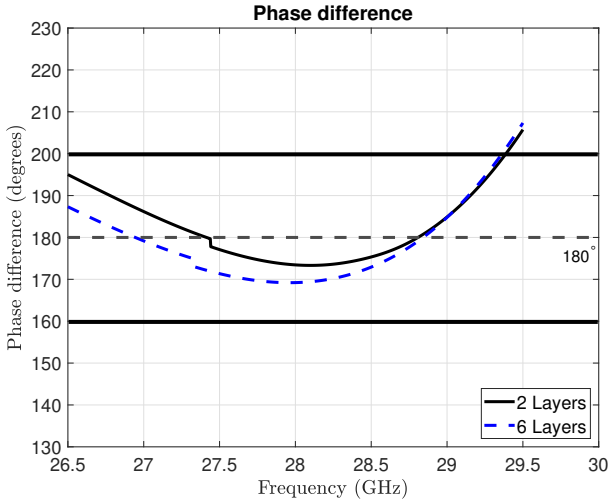

Fig. 7. Simulated phase difference between forward and reverse bias states for different PCB stack-ups.

the 4 different states, and their work concentrates over a single frequency. One noticeable trend is, due to the complexity of using p-i-n diodes in 2-bit architectures, the works using this architecture do not present dual-polarization capability.

TABLE I
COMPARISON BETWEEN THE UNIT-CELL PRESENTED IN THIS WORK WITH THE STATE-OF-THE-ART IN MMWAVE RIS.

Reference	Quantization	Band	Error	$\min(\lvert\Gamma\rvert)$	Polarization
[9]	1-bit	$28.2-30$ GHz	$20°$	-1.3 dB	Dual
[11]	1-bit	$27.5-29.5$ GHz	$36°$	-6 dB	Dual
[10]	2-bit	29 GHz	N/A	-2.12 dB	Single
[12]	2-bit	26.25 GHz	N/A	-17.83 dB	Single
This work	1-bit	$26.5-29.5$ GHz	$20°$	-1.8 dB	Dual

IV. CONCLUSION

This paper presented a novel 1-bit, dual-polarized unit-cell design capable of operating over the entire n257 5G mmWave band. This unique design showed remarkable performance with a phase difference error of $\pm 20°$ for almost the entirety of the 3 GHz band, whilst reflecting more than 80% of the energy. Considering the challenges of mmWave for 5G and beyond, such as path-loss and LoS requirements, the proposed unit-cell is suitable for RIS design, providing excellent performance to connect BS to UE due to its high reflectivity, phase accuracy and wide bandwidth. The former assists in reducing the losses on the reflective surface, and the latter in improving beam pointing accuracy, necessary in 1-bit systems to mitigate quantization losses. Numerical simulations point out that the unit-cell performs well on a 6-layer PCB stack-up, often necessary to improve signal integrity in RIS design. Finally, we provided a comparison with state-of-the-art unit-cells for RIS design, and our numerical results showed advantages over bandwidth, dual polarization operation and phase accuracy.

ACKNOWLEDGMENT

This work was supported by (i) the European Union Horizon 2020 project 6G-SANDBOX under grant agreement no. 101096328 and (ii) Department for the Economy of Northern Ireland under US Ireland R&D Partnership grant no. USI 199. The authors thank Mr Kieran Rainey for the technical support.

REFERENCES

[1] Y. Zhang, B. Di, H. Zhang, J. Lin, C. Xu, D. Zhang, Y. Li, and L. Song, "Beyond cell-free mimo: Energy efficient reconfigurable intelligent surface aided cell-free mimo communications," *IEEE Transactions on Cognitive Communications and Networking*, vol. 7, no. 2, pp. 412–426, 2021.

[2] Z. Yang, M. Chen, W. Saad, W. Xu, M. Shikh-Bahaei, H. V. Poor, and S. Cui, "Energy-efficient wireless communications with distributed reconfigurable intelligent surfaces," *IEEE Transactions on Wireless Communications*, vol. 21, no. 1, pp. 665–679, 2022.

[3] C. Huang, A. Zappone, G. C. Alexandropoulos, M. Debbah, and C. Yuen, "Reconfigurable intelligent surfaces for energy efficiency in wireless communication," *IEEE Transactions on Wireless Communications*, vol. 18, no. 8, pp. 4157–4170, 2019.

[4] G. Barb, F. Danuti, M. A. Ouamri, and M. Otesteanu, "Analysis of vegetation and penetration losses in 5g mmwave communication systems," in *2022 International Symposium on Electronics and Telecommunications (ISETC)*, 2022, pp. 1–5.

[5] H. Zhao, R. Mayzus, S. Sun, M. Samimi, J. K. Schulz, Y. Azar, K. Wang, G. N. Wong, F. Gutierrez, and T. S. Rappaport, "28 ghz millimeter wave cellular communication measurements for reflection and penetration loss in and around buildings in new york city," in *2013 IEEE International Conference on Communications (ICC)*, 2013, pp. 5163–5167.

[6] A. Araghi, M. Khalily, M. Safaei, A. Bagheri, V. Singh, F. Wang, and R. Tafazolli, "Reconfigurable intelligent surface (ris) in the sub-6 ghz band: Design, implementation, and real-world demonstration," *IEEE Access*, vol. 10, pp. 2646–2655, 2022.

[7] H. Yang, F. Yang, S. Xu, Y. Mao, M. Li, X. Cao, and J. Gao, "A 1-Bit 10x10 Reconfigurable Reflectarray Antenna: Design, Optimization, and Experiment," *IEEE Transactions on Antennas and Propagation*, vol. 64, no. 6, pp. 2246–2254, Jun. 2016.

[8] 3GPP, "ETSI TS 138 101-1," 2020.

[9] J. H. Oh, J. Jeong, Y. Park, and S.-H. Wi, "A 29 ghz Dual-Polarized Reconfigurable Intelligent Surface with 2-Dimensional Wide Scanning Range," in *2023 17th European Conference on Antennas and Propagation (EuCAP)*, 2023, pp. 1–5.

[10] Jeong, Jungi and Oh, Jun Hwa and Lee, Seung Yoon and Park, Yuntae and Wi, Sang-Hyuk, "An improved path-loss model for reconfigurable-intelligent-surface-aided wireless communications and experimental validation," *IEEE Access*, vol. 10, pp. 98 065–98 078, 2022.

[11] J.-B. Gros, V. Popov, M. A. Odit, V. Lenets, and G. Lerosey, "A Reconfigurable Intelligent Surface at mmWave Based on a Binary Phase Tunable Metasurface," *IEEE Open Journal of the Communications Society*, vol. 2, pp. 1055–1064, 2021.

[12] F. H. S. Fonseca, G. I. Morais, G. C. Clemente, and C. J. B. Pagan, "Tunable 2-bit Unit Cell Based in a Square Loop for Reconfigurable Intelligent Surface Application," in *2022 Asia-Pacific Microwave Conference (APMC)*, 2022, pp. 875–877.

[13] C. R. Wilke, "Quantization Effects of Beamforming in Desnse Phased Arrays," Ph.D. dissertation, Department of Electrical and Electronic Engineering, University of Stellenbosch, South Africa, Mar 2018. [Online]. Available: https://scholar.sun.ac.za/server/api/core/bitstreams/7802ed79-b1ed-4cc1-8edf-0d1e67e8b249/content